Birdstrike analysis of the wing slats of EF-2000

F. Rueda[1], F. Beltrán[1], C. Maderuelo[2] & H. Climent[2]
[1]*Advanced Design $ Analysis Division. Ingeniería IDOM, Spain*
[2]*Structural Dynamics, EADS-CASA, Spain*

Abstract

Aeroplanes have to meet a series of requirements regarding bird strike. Those requirements are defined basically in terms of structural resistance and the allowable degradation in flying qualities. One of the areas of the aircraft exposed to bird strike is the leading edge of the wing. The Eurofighter 2000 (EF-2000) is equipped with movable leading edge surfaces or “slats”. The requirements for the slats in relation with potential bird strikes is that birds should not penetrate the leading edge of the skin or, in case of penetration, no critical damage should be induced to the structural elements behind the skin.

For the EF-2000, the assessment of bird strike resistance of the slats has been based on numerical simulation of several impact scenarios covering a range of bird mass and velocity, points and sequences of impact and slat configurations.

The method of analysis is based on finite element simulation using the commercial explicit integration code PAM-CRASH. The model of the structure includes a representation with shell elements of the slats, the fittings and actuators and the relevant areas of the fixed leading edge of the wing. The most relevant features are the use of adaptive meshing for the shell elements and a strain rate dependent plasticity model (Johnson-Cook) for the materials.

The paper describes the basic assumptions of the analyses and the way in which the simulations have been carried out in an industrial environment. The paper also gives the main lines on how the results have been evaluated in order to assess the capacity of the slats to withstand the different impact scenarios.

1. Introduction

Collisions with birds pose a significant threat to the safety of aviation. Since 1960, about 400 aircraft have been destroyed and over 370 people killed as a result of bird and other wildlife strikes (Stevens [1]). Therefore, the airworthiness certification of an aircraft requires an specific level of birdstrike resistance.

The requirements to be met by the slats of the Eurofighter 2000 (EF-2000) regarding bird strike are defined in terms of structural resistance, the allowable degradation in flying qualities and the necessary measures to ensure that the debris will be within engine ingestion limits.

In the EF-2000, the assessment of the movable leading edges of the wing ("slats") under birdstrike loads has been based on an extensive series of numerical simulations. The simulations have covered a wide range of impact sequences and locations, as well as bird masses and velocities. The assessment includes the definition of the worst case scenario, the verification that the specified requirements are met and the acquisition of a deep insight into the behaviour of the component.

This paper describes the basic assumptions of the analyses and how the simulations have been carried out in an industrial environment.

The rest of the paper is organised into five additional sections. First, a brief description of the component is given and the main aspects of the dynamic problem are outlined. Then, the numerical model used for the simulations is presented and discussed. Afterwards, an overview of the structural response of the slats under impact is given. Finally, a set of conclusions and a list of references are included.

2. Description of the Problem

Description of the Structure

The slats of the EF-2000 are movable leading edge surfaces which operate at fixed positions from fully retracted to fully extended. They are divided into two sections, inboard and outboard. These sections are one-piece titanium parts manufactured by diffusion bonding and superplastic forming (DB-SPF). Basically, each slat consists of the upper, lower and nose skin, a spar and a series of ribs.

The inboard slat has a total length of 2450 mm, with a chord that varies between 115 and 160 mm (figure 1). The height of the spar in a typical section is about 70 mm. The length of the outboard slat is approximately of 2720 mm, with a chord between 57 and 115 mm and a typical height of the spar around 58 mm.

The connection between the slats and the fixed part of the wing is provided by means of three tracks and two actuators per slat (figure 1). The tracks are curved titanium I beams that slide on a set of rollers attached to guiding ribs. These ribs are at the fixed part of the wing (D-nose). The tracks are connected to the slat spar by means of two riveted fittings. The actuators join the slat spar with the front spar of the wing, moving the slat back and forth. The connections are also riveted.

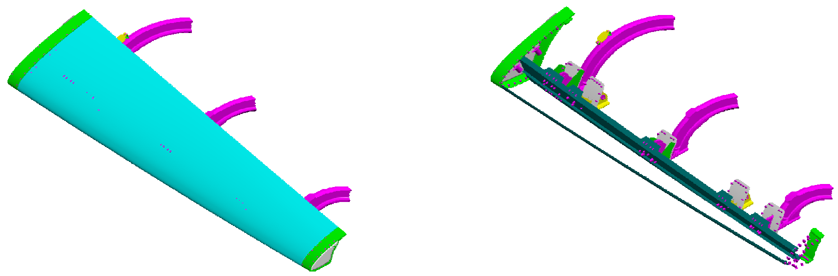

Figure 1: General view of the outboard slat with and without skin and ribs.

The leading edge of the fixed part of the wing (D-nose) lies directly underneath the slats. It consists of a carbon fibre composite spar, and ribs and skin panels made of aluminium (figure 2).

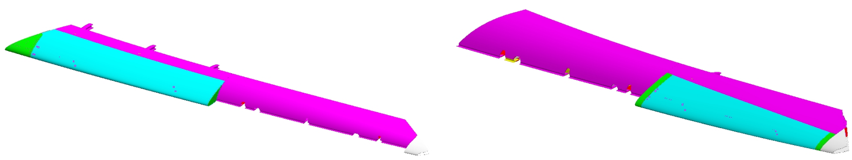

Figure 2: General view of the inboard and outboard slats and their assembly with the D-nose.

Basic assumptions

Some general considerations concerning the assumptions made in the numerical simulations of bird impacts serve as an introduction to the nature of the problem:

- The analysis is transient and non-linear. The sources of non-linearity are the large deformations and displacements, the constraints derived from contacts and the elastic-plastic behaviour considered for the materials.
- Strain rate dependent plasticity (Johnson-Cook model) has been considered for the material of the slat.
- Rivets at the fittings that join the slats with tracks and actuators have been introduced in the finite element model as point connections between meshed parts. The connections are set at the actual nominal position of the rivets. Rivet rupture is taken into account during the simulations.
- The front spar of the fixed part of the wing (D-nose) has been assumed fixed (i.e. no displacement) at the sections where the spar intersects with the ribs of the wing.
- The bird has been represented by an equivalent mass of water.

- The transient response has been computed using explicit integration of equations of motion.

Impact Scenarios

A number of different impact scenarios have been simulated in order to identify the worst case scenario and to get a deep insight into the behaviour of the component. The main points subjected to variation for both the inboard and outboard slats have been:

- Slat configuration: retracted, partially deployed or fully deployed
- Impact point along the length of the slat.
- Impact sequence: one single bird strike, two birds impacting simultaneously or three birds impacting at the same point consecutively.
- Bird mass: birds of 0.5 kg and 1.0 kg.
- Bird speed: 180.1 m/s, 257.3 m/s and 295.9 m/s.
- Bird shape: ellipsoidal and cylindrical shapes assigned to the mass of water used to represent the bird.
- Material constitutive parameters, such as the dependence of yield stress on strain rate and the failure strain of the titanium alloy.

As a result of this, a battery of 51 simulations has been carried out in order to acquire an acceptable basis to determine where the most severe effects are to be expected.

The initial velocity of the birds is always parallel to the longitudinal axis of the aircraft. The most of selected impact points are at the chord plane, with some additional points at the skin above the spar of the slat.

3. Numerical Model

Structural model

Six finite element models have been generated from CAD models, corresponding to the inboard and outboard slats, fully retracted, partially extended and fully deployed.

In each case, the model of the structure includes the slat structure (skin, spar and ribs), the two formed end ribs, the fittings for track and actuator connection, the tracks, the actuators, the rollers and the relevant parts of the D-nose.

The structure of the slat has been idealised using four node shell finite elements, with reduced integration and hourglass control. In areas in which intensive plastification is expected, five integration points through the thickness have been used. In the rest of the model, three integration points have been considered adequate.

Since the expected effects of the impacts are essentially of a local nature, the finite element meshes have been designed for producing a good approximation of the deformation in the impact areas, specially in the skin and the spar of the slats. In addition, the adaptive meshing facility of PAM-CRASH (PAM SYSTEM, 2000 [2]) has been used. Therefore, the simulations have been able to capture accurately the very localised deformations (folds) that take place in the nose skin during the impacts. For an average initial element size of about 8 mm, adaptive meshing has produced in this area elements with sides in the order of the thickness of the shells, that is, of about 2 mm.

The initial meshes corresponding to the inboard slat include 24000 nodes. The number of nodes in the initial meshes corresponding to the outboard slat is 31000 (figures 3 to 5).

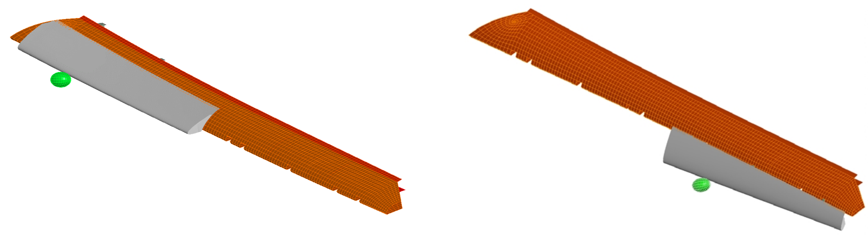

Figure 3. Overall view of the model for bird impacts on inboard slat (fully retracted) and outboard slat (fully deployed)

The actuators have been introduced in the model as beam elements. Twenty elements per actuator have been used in order to get a good representation of stress waves moving along the component. The ends of the actuators have been connected to the rest of the model using rigid body constraints.

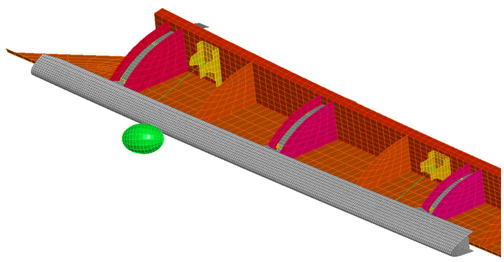

Figure 4: Initial mesh for bird impacts on inboard slat fully retracted. Detail of nose skin and slat/D-nose assembly

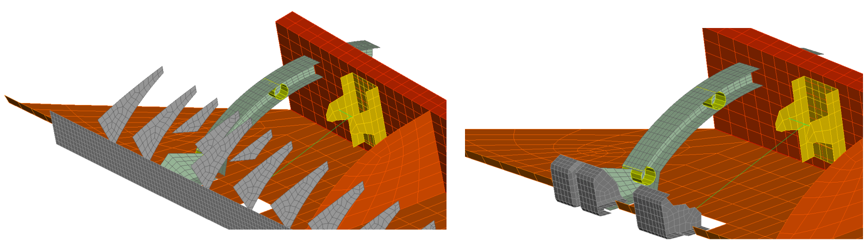

Figure 5: Initial mesh for bird impacts on inboard slat fully retracted: (I) Detail of spar and ribs, (II) Detail of track, rollers, actuator and fittings

Bird model

During impacts that take place at several hundreds of metres per second, the usual practice in finite element analysis is to represent the bird using an equivalent mass of water. The reason is that during these high-speed impacts, all forces associated to the bird internal structure are negligible when compared with inertia forces. A correct representation of the mass of the bird is the key aspect of the bird representation.

The second aspect that influences the development of the bird-structure interaction forces is the bird material compressibility. The compressibility determines the time history of the interaction forces. Considering the bird compressibility equal to that of water is conservative, since it produces a "harder" impact, but not excessively conservative, since water makes up to 2/3 of bird tissues. Increasing the bird compressibility would make the impact "softer" and slightly longer, reducing the magnitude of interaction forces at each instant.

The bird material has been introduced into the model as a perfect fluid, with a linear equation of state. The bird has been represented using six node and eight node solid elements, with reduced integration and hourglass control. In the computations, distortion of the bird is exclusively resisted by hourglass control forces.

Material constitutive models

An elastic-plastic model with damage has been used for the metallic parts.

The slats are made of a titanium alloy, as well as the tracks and the fittings for track and actuator connection. On the other hand, the skin panels of the D-nose and the guiding ribs are made of aluminium.

The mechanical behaviour of the titanium alloy is relatively sensitive to the strain rate. The dependence of yield stress on strain rate has been determined by Macdougall and Harding using Hopkinson bar tests (Macdougall & Harding, [3]). The results reported in this reference have been used to match the parameters p and D of a Johnson-Cook model:

$$\sigma_n = \sigma_y \left[1 + p^{-1} \ln (\varepsilon'/D)\right] \tag{1}$$

where:

σ_n = yield stress at an effective strain rate of ε'

σ_y = yield stress at a strain rate of D

ε' = effective strain rate

p, D = material parameters

Strain rate dependence effects have been neglected for the rest of materials in the finite element model.

A damage model has been introduced for all the materials. The elements are eventually eliminated from the mesh when a certain level of effective plastic strain for each material is reached at least in one of the integration points through the thickness

Constraints and boundary conditions

The boundary conditions restrain the movement of the nodes of the D-nose spar that are closer to the main ribs of the wing. At this nodes all displacements and rotations have been set to zero.

On the other hand, a number of possible contacts have been declared in the finite element models. This set of contacts includes the contact of the bird with the skin, the contact of the nose skin with the spar, the self contact of the nose skin, the contact of the upper and lower skin of the slat, the contact of the lower skin of the slat with the D-nose and the contact of all the fittings with the parts they connect. In all these contacts, a dynamic friction coefficient of 0.15 has been assumed. A non-frictional contact has been declared between the external surface of the rollers and the corresponding tracks.

4. Results

The computer simulations have produced a large amount of information whose main features will be summarised in the present section. Figure 6 shows the impact sequence in one of the scenarios analysed for the inboard slat.

The first thing that should be said is that the damage produced to the slats is local in nature (figure 7). Only a small portion of the span of the slat is affected by each bird. The damage concentrates in the nose skin. The spar of the slat, especially in the outboard slat, is the next part in the hierarchy of damage, whereas the rest of components basically remain in the elastic range, that is, without unrecoverable deformation.

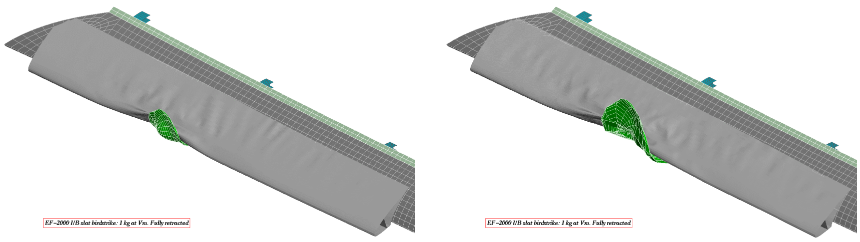

Figure 6: Impact at 1.0 ms and at end of calculation (2.0 ms) for a typical impact scenario

The simulations show that the slats are able to withstand the specified impacts without the birds penetrating the nose skin. As it could be expected, the severity of the impact increases with the initial velocity of the birds, but the mechanism of damage is similar in all cases. Due to the sweepback angle of the leading edge, the bird tends to slide in the outboard direction and produces an oblong dent in the nose skin. A consequence of this sliding of the bird is that the area of the skin that interacts with the bird changes along the time of the impact. Therefore, the damage to the skin tends to be distributed over an area larger than the area of initial contact.

As shown in figure 8, the shape of the dent in the skin is different depending on the configuration of the slat, fully retracted or deployed. When the slat is fully retracted, the dent has a crater like shape whose perimeter can go beyond the slat spar, up to the limit of the ribs. On the other hand, when the slat is deployed, the bird turns down the nose skin, producing just a large fold below the bird. In both cases, the stiffening role played by the slat ribs prevents the overall downward movement from causing more severe damage.

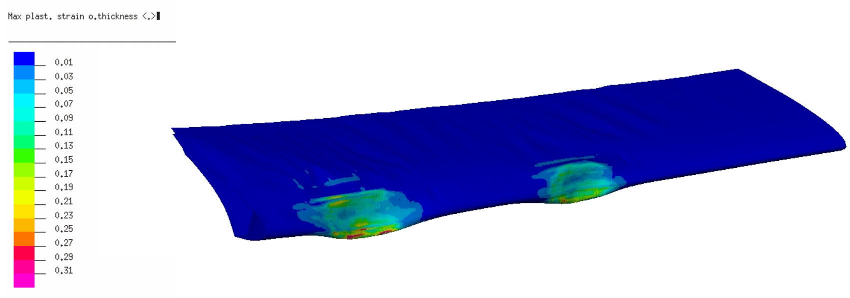

Figure 7: Contour of max. effective plastic strain for a scenario involving two simultaneous impacts

At the perimeter of the dent, the metal of the skin develops very sharp folds and, eventually, bending cracks. These are, as a rule, the only areas in which the simulations predict the rupture of the material (figures 9 and 10). These areas appear in red within the contour picture of figure 10 (maximum effective plastic strain), where the level of refinement provided by the adaptive meshing speaks for itself.

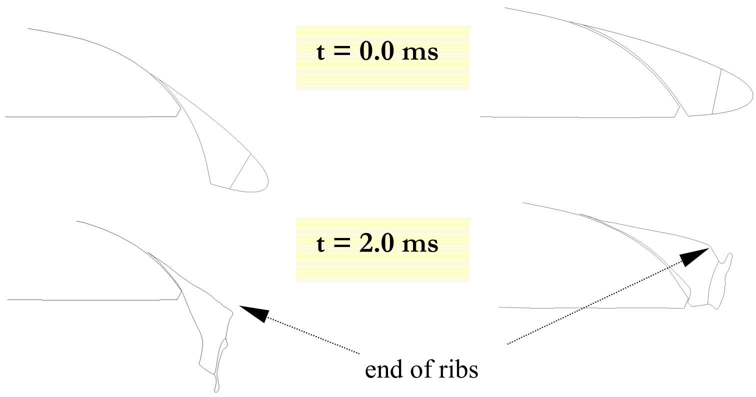

Figure 8: Schematic view of impact effects for slats deployed and retracted

The spar of the slat experiences local damage in the area around the impact point. This damage is far less severe than the damage to the nose skin and it is located mainly along the weld line of the spar with the skin. In this area, some plastic deformation is to be expected but, except for some extreme scenarios, no cracks develop (figure 11).

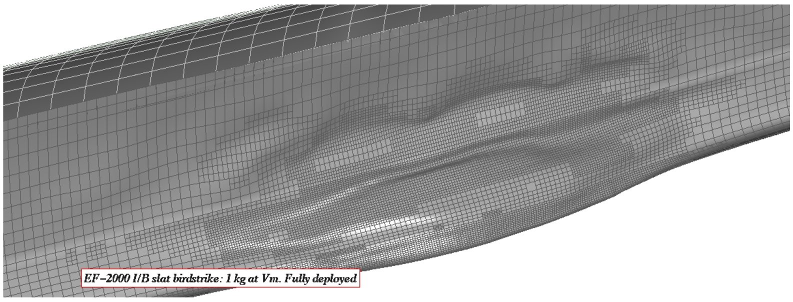

Figure 9: Detail of the deformed mesh for a typical impact scenario

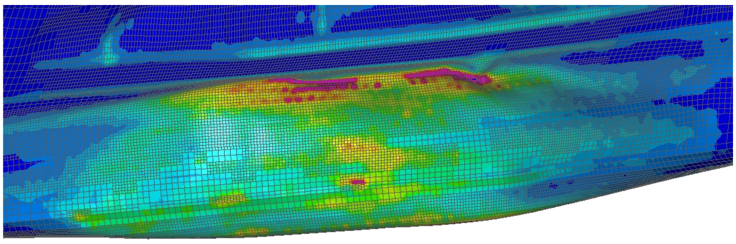

Figure 10: Contour of max. effective plastic strain in the nose of the slat for a typical impact scenario

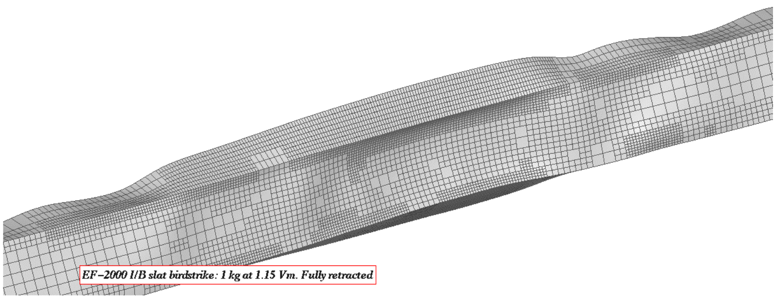

Figure 11: Detail of the deformed mesh (spar) for a typical impact scenario

Finally, the elements of the D-nose of the wing, skin, ribs and the front spar of the wing, hardly experience any damage.

Figure 12 shows the final deformed mesh corresponding to one of the worst scenarios: the impact of three consecutive birds on the outboard slat fully deployed.

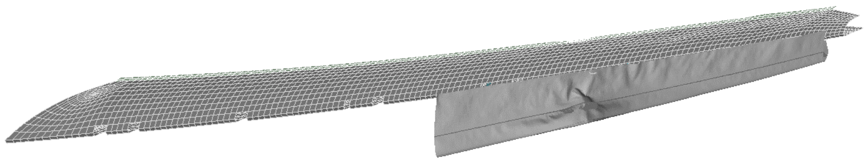

Figure 12: Overall view of the deformed mesh for an impact in the outboard slat fully deployed

5. Conclusions

The structural behaviour under bird strike loads of the slats corresponding to the production version of the EF-2000 has been assessed. The assessment has been based on extensive computer simulation of a set of impact scenarios, covering different bird masses and initial speeds, as well as different impact points and positions of the slats. From the computer simulations, a good understanding of the slat behaviour has been gained.

From a the analyst's point of view, it has to be mentioned that the adaptive meshing facility of the software has been specially helpful for capturing the very localised deformation that takes place around impact locations. Another point is that, at these relatively high impact speeds, the results are almost insensitive to the initial shape of the bird representation, as long as the mass and the length are maintained. Finally, the importance of taking into account strain rate sensitivity should also be remarked. In this particular case, if this effect had been neglected, unrealistic high levels of damage would have been predicted.

6. References

[1] Stevens. R., Enhancing aviation safety through research & development. *Office of Aviation Research. 68th NASAO Annual Convention.* September 1999. (www.aero-space.nasa.gov/library/nasao/safety).

[2] PAM SYSTEM International. "PAM-CRASH/PAM-SAFE Solver Notes Manual". Version 2000.

[3] Macdougall, D.A.S. & Harding, J., A constitutive relation and failure criterion for Ti6Al4V alloy at impact rates of strain. *Journal of Mechanics and Physics of Solids*, **47**, pp. 1157-1185, 1999.